Supplementary Information for

# Tuneable Phase Behaviour and Glass Transition via Polymerization-Induced Phase Separation in Crosslinked Step-Growth Polymers

Samuel C. Leguizamon[a]; Juhong Ahn[b]; Sangwoo Lee[b]; Brad H. Jones[a,*]

[a] Department of Organic Materials Science, Sandia National Laboratories, Albuquerque, NM, 87185, USA

[b] Department of Chemical and Biological Engineering, Rensselaer Polytechnic Institute, Troy, NY, 12180, USA

**Experimental Section:**

**Materials and Sample Preparation.** Triethylenetetramine (TETA) and poly(ethylene glycol) diamine (PEG, $M_w$ 2000) were obtained from Millipore Sigma (Burlington, MA USA). Jeffamines D230, D2000, and T3000 were obtained from Huntsman Corporation. EPON 828, a diglycidyl ether of bisphenol A (DGEBA), was obtained from Miller-Stephenson (Sylmar, CA USA). D.E.R. 732 (DER) was obtained from Palmer Holland (North Olmsted, OH USA). All reagents were used as received.

Mixtures of DGEBA and curing agents bearing epoxy or amine functional groups, respectively, were prepared so that epoxies and amine hydrogens were kept at a constant stoichiometric ratio (*i.e.*, $r = [-NH-]_{0,total} / [epoxide]_{0,total} = 1$), while the fraction of amine hydrogens from T3000 was varied and defined by the value $m = [-NH-]_{0,T3000}/[-NH-]_{0,total}$, where $[-NH-]_{0,T3000}$ and $[-NH-]_{0,total}$ are the initial molar concentrations of T3000 amine hydrogens and total amine hydrogens in the mixture, respectively. The remaining amine hydrogens were provided by curing agents with concentrations described by $n = [-NH-]_{0,TETA}/([-NH-]_{0,D230} + [-NH-]_{0,TETA})$, where $[-NH-]_{0,D230}$ and $[-NH-]_{0,TETA}$ are the initial molar concentrations of amine hydrogens from the binary curing agent mixture. Similarly, mixtures incorporating DER 732, PEG, and/or D2000 were kept at a constant stoichiometric ratio (*i.e.*, $r = [-NH-]_{0,total} / [epoxide]_{0,total} = 1$), while the fraction of amine hydrogens from rubbers was varied to account for a mole fraction of 0.1 in total. In the DER-DGEBA-T3000-TETA system, the total epoxy functional groups was kept constant but attributing epoxy-bearing species were varied by $e = [epoxide]_{0,DER732}/([epoxide]_{0,DGEBA} + [epoxide]_{0,DER732})$, where $[epoxide]_{0,DGEBA}$ and $[epoxide]_{0,DER732}$ are the initial molar concentrations of epoxides from the binary epoxide mixture. In the DGEBA-PEG-D2000-TETA system, the amine hydrogens from rubbers were described by $R = [-NH-]_{0,D2000}/([-NH-]_{0,PEG} +$

$[-NH-]_{0,D2000}$), where $[-NH-]_{0,PEG}$ and $[-NH-]_{0,D2000}$ are the initial molar concentrations of amine hydrogens from the binary rubber mixture

Desired amounts of amine bearing species defined by *n*, *m,* and/or *R* were mixed in a Thinky planetary centrifugal mixer prior to addition of DGEBA and/or DER 732 and a second round of centrifugal mixing. The homogeneous, uncured liquid was then spread into a silicone mold to obtain the desired shape for mechanical testing (i.e., rectangular plaques). The cure temperature was controlled by placing the silicone mold in a temperature-controlled oven, yielding thin, solid, rectangular plaques that were easily demolded from the mold cavity. Previous work showed there is no dependence on final morphology or thermomechanical properties on cure temperature below 140°C,[1] therefore samples in this study were cured isothermally at 100°C for 24h and compared with the previous samples cured at 60°C.

Formulations are shown in Table S1.

**Dynamic Mechanical Analysis (DMA).** DMA was performed using a strain-controlled Rheometric Scientific (Piscataway, NJ, USA) ARES-LS/M rheometer operating in small-amplitude oscillatory shear. The dynamic shear storage ($G'$) and loss ($G''$) moduli and loss tangent ($G''/G'$) of the thin rectangular plaques described above were measured using torsional deformation with 1 Hz oscillation frequency, 0.5% strain amplitude, and a ramp rate of 3°C/min. Measurements were conducted upon heating from 25°C to 200°C, followed by subsequent cooling from 200°C to -75°C. The samples were assumed to be fully cured after heating to 200°C, thus data are presented from the cooling cycle unless otherwise noted.

**X-ray Scattering.** Small- and wide-angle X-ray scattering (SWAXS) characterization of the thermosets was conducted at the 12-ID beamline at the National Synchrotron Light Source-II

(NSLS-II), Brookhaven National Laboratory, NY. Two-dimensional (2D) scattering patterns were recorded using Pilatus 1M and 300kW and 300kW detectors (Dectris, Switzerland) located at 8,300 mm and 275 mm away from the sample, respectively. The reciprocal space over the scattering vector $q = 4\pi \cdot \sin(\theta/2)/\lambda$ from 0.003 $Å^{-1}$ to 5 $Å^{-1}$ where the $\theta$ is the scattering angle and $\lambda = 0.8920$ Å was interrogated for the structure analysis. All sample measurements were conducted under vacuum (< $10^{-3}$ Torr) at 25 °C unless noted otherwise.

The time resolved X-ray scattering characterization over the DGEBA-T3000-D230-TETA sample under curing was conducted using the HFSX350 capillary stage (Linkam). The precursor solutions of the samples were prepared at 25 °C by mixing DGEBA and curing agents, the mixtures were immediately loaded in quartz capillaries of the nominal diameter of 1.5 mm (Charles-Supper), sealed using bee waxes (Hampton Research), and the time-resolved X-ray-scattering measurements were conducted at elevated temperatures.

**Table S1.** Formulations investigated in this work defined by *n*, *m*, *e*, and *R* with wt% of each reagent shown.

| *m* | *n* | DGEBA wt% | T3000 wt% | TETA wt % | D230 wt % |
|---|---|---|---|---|---|
| 0.025 | 0 | 73.3 | 4.9 | 0.0 | 21.8 |
| 0.025 | 0.1 | 74.3 | 4.9 | 0.9 | 19.9 |
| 0.025 | 0.2 | 75.2 | 5.0 | 1.9 | 17.9 |
| 0.025 | 0.3 | 76.2 | 5.1 | 2.9 | 15.9 |
| 0.025 | 0.4 | 77.2 | 5.1 | 3.9 | 13.8 |
| 0.025 | 0.5 | 78.2 | 5.2 | 4.9 | 11.6 |
| 0.025 | 0.6 | 79.3 | 5.3 | 6.0 | 9.4 |
| 0.025 | 0.7 | 80.4 | 5.3 | 7.1 | 7.2 |
| 0.025 | 0.8 | 81.5 | 5.4 | 8.2 | 4.8 |
| 0.025 | 0.9 | 82.7 | 5.5 | 9.4 | 2.5 |
| 0.025 | 1 | 83.9 | 5.6 | 10.6 | 0.0 |
| 0.1 | 0 | 64.9 | 17.2 | 0.0 | 17.8 |
| 0.1 | 0.1 | 65.6 | 17.4 | 0.8 | 16.2 |
| 0.1 | 0.2 | 66.3 | 17.6 | 1.5 | 14.6 |
| 0.1 | 0.3 | 67.0 | 17.8 | 2.3 | 12.9 |
| 0.1 | 0.4 | 67.7 | 18.0 | 3.2 | 11.2 |
| 0.1 | 0.5 | 68.5 | 18.2 | 4.0 | 9.4 |
| 0.1 | 0.6 | 69.2 | 18.4 | 4.8 | 7.6 |
| 0.1 | 0.7 | 70.0 | 18.6 | 5.7 | 5.8 |
| 0.1 | 0.8 | 70.8 | 18.8 | 6.6 | 3.9 |
| 0.1 | 0.9 | 71.6 | 19.0 | 7.5 | 2.0 |
| 0.1 | 1 | 72.4 | 19.2 | 8.4 | 0.0 |

| *m* | *n* | DGEBA wt% | T3000 wt% | TETA wt % | D230 wt % |
|---|---|---|---|---|---|
| 0.2 | 0 | 56.4 | 29.9 | 0.0 | 13.8 |
| 0.2 | 0.1 | 56.8 | 30.1 | 0.6 | 12.5 |
| 0.2 | 0.2 | 57.3 | 30.4 | 1.2 | 11.2 |
| 0.2 | 0.3 | 57.7 | 30.6 | 1.8 | 9.9 |
| 0.2 | 0.4 | 58.2 | 30.9 | 2.4 | 8.5 |
| 0.2 | 0.5 | 58.7 | 31.1 | 3.0 | 7.2 |
| 0.2 | 0.6 | 59.2 | 31.4 | 3.7 | 5.8 |
| 0.2 | 0.7 | 59.7 | 31.7 | 4.3 | 4.4 |
| 0.2 | 0.8 | 60.2 | 31.9 | 5.0 | 2.9 |
| 0.2 | 0.9 | 60.7 | 32.2 | 5.6 | 1.5 |
| 0.2 | 1 | 61.2 | 32.5 | 6.3 | 0.0 |
| 0.3 | 0 | 49.8 | 39.6 | 0.0 | 10.6 |
| 0.3 | 0.1 | 50.1 | 39.8 | 0.5 | 9.6 |
| 0.3 | 0.2 | 50.4 | 40.1 | 0.9 | 8.6 |
| 0.3 | 0.3 | 50.7 | 40.3 | 1.4 | 7.6 |
| 0.3 | 0.4 | 51.0 | 40.6 | 1.8 | 6.5 |
| 0.3 | 0.5 | 51.3 | 40.9 | 2.3 | 5.5 |
| 0.3 | 0.6 | 51.7 | 41.1 | 2.8 | 4.4 |
| 0.3 | 0.7 | 52.0 | 41.4 | 3.3 | 3.3 |
| 0.3 | 0.8 | 52.3 | 41.6 | 3.8 | 2.2 |
| 0.3 | 0.9 | 52.7 | 41.9 | 4.3 | 1.1 |
| 0.3 | 1 | 53.0 | 42.2 | 4.8 | 0.0 |

| *m* | *n* | DGEBA wt% | T3000 wt% | TETA wt % | D230 wt % |
|---|---|---|---|---|---|
| 0.4 | 0 | 44.6 | 47.3 | 0.0 | 8.2 |
| 0.4 | 0.1 | 44.8 | 47.5 | 0.3 | 7.4 |
| 0.4 | 0.2 | 45.0 | 47.7 | 0.7 | 6.6 |
| 0.4 | 0.3 | 45.2 | 48.0 | 1.1 | 5.8 |
| 0.4 | 0.4 | 45.4 | 48.2 | 1.4 | 5.0 |
| 0.4 | 0.5 | 45.6 | 48.4 | 1.8 | 4.2 |
| 0.4 | 0.6 | 45.9 | 48.7 | 2.1 | 3.4 |
| 0.4 | 0.7 | 46.1 | 48.9 | 2.5 | 2.5 |
| 0.4 | 0.8 | 46.3 | 49.1 | 2.9 | 1.7 |
| 0.4 | 0.9 | 46.5 | 49.4 | 3.2 | 0.9 |
| 0.4 | 1 | 46.8 | 49.6 | 3.6 | 0.0 |
| 0.5 | 0 | 40.3 | 53.5 | 0.0 | 6.2 |
| 0.5 | 0.1 | 40.5 | 53.7 | 0.3 | 5.6 |
| 0.5 | 0.2 | 40.6 | 53.9 | 0.5 | 5.0 |
| 0.5 | 0.3 | 40.8 | 54.1 | 0.8 | 4.4 |
| 0.5 | 0.4 | 40.9 | 54.3 | 1.1 | 3.7 |
| 0.5 | 0.5 | 41.1 | 54.5 | 1.3 | 3.1 |
| 0.5 | 0.6 | 41.2 | 54.7 | 1.6 | 2.5 |
| 0.5 | 0.7 | 41.4 | 54.9 | 1.9 | 1.9 |
| 0.5 | 0.8 | 41.5 | 55.1 | 2.1 | 1.3 |
| 0.5 | 0.9 | 41.7 | 55.3 | 2.4 | 0.6 |
| 0.5 | 1 | 41.8 | 55.5 | 2.7 | 0.0 |

| *m* | *n* | DGEBA wt% | T3000 wt% | TETA wt % | D230 wt % |
|---|---|---|---|---|---|
| 0.6 | 0.0 | 36.9 | 58.7 | 0.0 | 4.5 |
| 0.6 | 0.1 | 36.9 | 58.8 | 0.2 | 4.1 |
| 0.6 | 0.2 | 37.0 | 59.0 | 0.4 | 3.6 |
| 0.6 | 0.3 | 37.1 | 59.1 | 0.6 | 3.2 |
| 0.6 | 0.4 | 37.2 | 59.3 | 0.8 | 2.7 |
| 0.6 | 0.5 | 37.3 | 59.4 | 1.0 | 2.3 |
| 0.6 | 0.6 | 37.4 | 59.6 | 1.2 | 1.8 |
| 0.6 | 0.7 | 37.5 | 59.7 | 1.4 | 1.4 |
| 0.6 | 0.8 | 37.6 | 59.9 | 1.6 | 0.9 |
| 0.6 | 0.9 | 37.7 | 60.1 | 1.8 | 0.5 |
| 0.6 | 1.0 | 37.8 | 60.2 | 2.0 | 0.0 |
| 0.7 | 0.0 | 33.9 | 63.0 | 0.0 | 3.1 |
| 0.7 | 0.1 | 34.0 | 63.1 | 0.1 | 2.8 |
| 0.7 | 0.2 | 34.0 | 63.2 | 0.3 | 2.5 |
| 0.7 | 0.3 | 34.1 | 63.3 | 0.4 | 2.2 |
| 0.7 | 0.4 | 34.2 | 63.4 | 0.5 | 1.9 |
| 0.7 | 0.5 | 34.2 | 63.5 | 0.7 | 1.6 |
| 0.7 | 0.6 | 34.3 | 63.7 | 0.8 | 1.3 |
| 0.7 | 0.7 | 34.3 | 63.8 | 0.9 | 0.9 |
| 0.7 | 0.8 | 34.4 | 63.9 | 1.1 | 0.6 |
| 0.7 | 0.9 | 34.5 | 64.0 | 1.2 | 0.3 |
| 0.7 | 1.0 | 34.5 | 64.1 | 1.3 | 0.0 |

| *m* | *n* | DGEBA wt% | T3000 wt% | TETA wt % | D230 wt % |
|---|---|---|---|---|---|
| 0.8 | 0 | 31.4 | 66.7 | 0.0 | 1.9 |
| 0.8 | 0.1 | 31.5 | 66.7 | 0.1 | 1.7 |
| 0.8 | 0.2 | 31.5 | 66.8 | 0.2 | 1.5 |
| 0.8 | 0.3 | 31.5 | 66.9 | 0.2 | 1.3 |
| 0.8 | 0.4 | 31.6 | 67.0 | 0.3 | 1.2 |
| 0.8 | 0.5 | 31.6 | 67.0 | 0.4 | 1.0 |
| 0.8 | 0.6 | 31.6 | 67.1 | 0.5 | 0.8 |
| 0.8 | 0.7 | 31.7 | 67.2 | 0.6 | 0.6 |
| 0.8 | 0.8 | 31.7 | 67.3 | 0.7 | 0.4 |
| 0.8 | 0.9 | 31.7 | 67.3 | 0.7 | 0.2 |
| 0.8 | 1 | 31.8 | 67.4 | 0.8 | 0.0 |
| 0.9 | 0 | 29.3 | 69.8 | 0.0 | 0.9 |
| 0.9 | 0.1 | 29.3 | 69.9 | 0.0 | 0.8 |
| 0.9 | 0.2 | 29.3 | 69.9 | 0.1 | 0.7 |
| 0.9 | 0.3 | 29.3 | 70.0 | 0.1 | 0.6 |
| 0.9 | 0.4 | 29.3 | 70.0 | 0.2 | 0.5 |
| 0.9 | 0.5 | 29.3 | 70.0 | 0.2 | 0.4 |
| 0.9 | 0.6 | 29.3 | 70.1 | 0.2 | 0.4 |
| 0.9 | 0.7 | 29.4 | 70.1 | 0.3 | 0.3 |
| 0.9 | 0.8 | 29.4 | 70.1 | 0.3 | 0.2 |
| 0.9 | 0.9 | 29.4 | 70.2 | 0.3 | 0.1 |
| 0.9 | 1 | 29.4 | 70.2 | 0.4 | 0.0 |

| *m* | *e* | DGEBA wt% | DER 732 wt% | T3000 wt% | TETA wt % |
|---|---|---|---|---|---|
| 0.1 | 0 | 0.0 | 81.6 | 12.8 | 5.6 |
| 0.1 | 0.1 | 5.0 | 76.0 | 13.2 | 5.8 |
| 0.1 | 0.2 | 10.3 | 70.0 | 13.7 | 6.0 |
| 0.1 | 0.3 | 16.0 | 63.5 | 14.2 | 6.2 |
| 0.1 | 0.4 | 22.2 | 56.6 | 14.7 | 6.5 |
| 0.1 | 0.5 | 28.9 | 49.1 | 15.3 | 6.7 |
| 0.1 | 0.6 | 36.1 | 40.9 | 16.0 | 7.0 |
| 0.1 | 0.7 | 44.0 | 32.0 | 16.7 | 7.3 |
| 0.1 | 0.8 | 52.6 | 22.3 | 17.4 | 7.6 |
| 0.1 | 0.9 | 62.0 | 11.7 | 18.3 | 8.0 |
| 0.1 | 1 | 72.4 | 0.0 | 19.2 | 8.4 |

| *m* | *R* | DGEBA wt% | PEG wt% | D2000 wt % | TETA wt % |
|---|---|---|---|---|---|
| 0.1 | 0 | 72.4 | 19.2 | 0.0 | 8.4 |
| 0.1 | 0.1 | 72.4 | 17.3 | 1.9 | 8.4 |
| 0.1 | 0.2 | 72.4 | 15.4 | 3.8 | 8.4 |
| 0.1 | 0.3 | 72.4 | 13.4 | 5.8 | 8.4 |
| 0.1 | 0.4 | 72.4 | 11.5 | 7.7 | 8.4 |
| 0.1 | 0.5 | 72.4 | 9.6 | 9.6 | 8.4 |
| 0.1 | 0.6 | 72.4 | 7.7 | 11.5 | 8.4 |
| 0.1 | 0.7 | 72.4 | 5.8 | 13.4 | 8.4 |
| 0.1 | 0.8 | 72.4 | 3.8 | 15.4 | 8.4 |
| 0.1 | 0.9 | 72.4 | 1.9 | 17.3 | 8.4 |
| 0.1 | 1 | 72.4 | 0.0 | 19.2 | 8.4 |

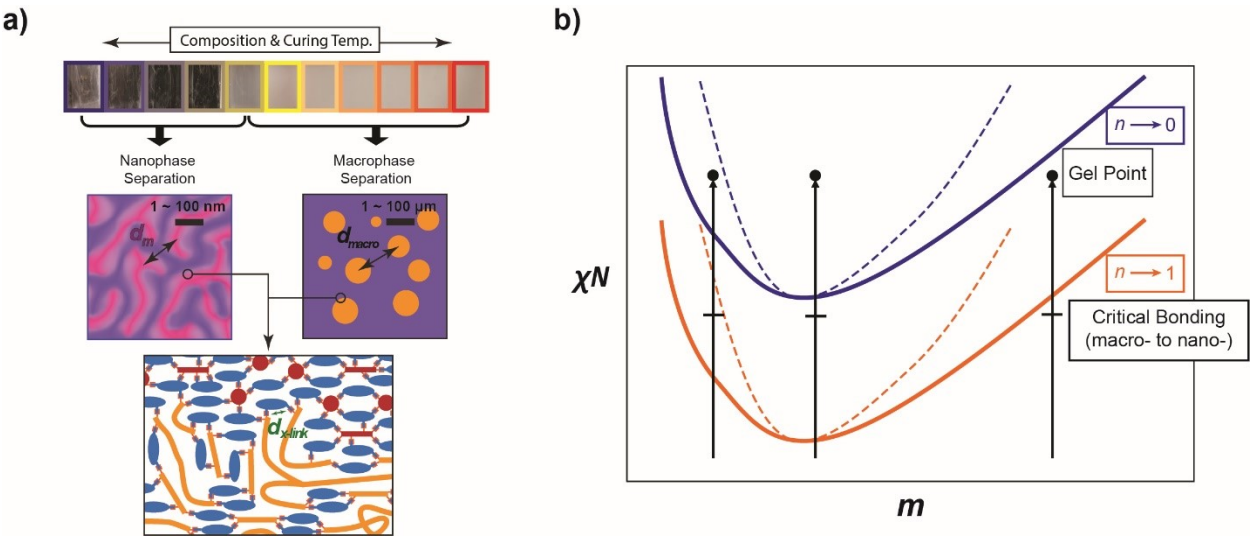


**Figure S1. Schematic illustrations of phase separation process in CA-tuned epoxies.** (a) Nanophase separation and macrophase separation into domains defined by characteristic length scales $d_m$ and $d_{macro}$, respectively. The expanded area shows a cartoon representation of the domain interfaces with blue ovals, red circles/lines, and yellow lines indicating the epoxy, binary CA, and rubber components of the network, respectively. $d_{x\text{-}link}$ is the characteristic length scale of the highly crosslinked domains. (b) A generalized representation of the impact of mixture composition on the curing and phase separation in the context of classic Flory-Huggins phase space. $\chi N$ is the product of the Flory-Huggins interaction parameter and the degree of polymerization of the network, *i.e.*, the extent of epoxide conversion. The solid blue and orange lines indicate a binodal curve for smaller and larger $n$, respectively, while the dotted blue and orange lines indicate the corresponding spinodal curves. At smaller $n$, the epoxy-CA network is more compatible with the rubber (mean $\chi$ decreases in the pseudo-binary phase diagram of $\chi N$ and $m$ of the panel b), thus a larger $N$ is needed to cross the phase boundary. At larger $n$, the epoxy-CA network is less compatible with the rubber (mean $\chi$ increases), thus a smaller $N$ is needed to cross the phase boundary. Each arrow represents the cure of a mixture with different rubber content $m$, starting at $N = 1$ and curing through the gel (or vitrification) point, at which phase separation is arrested. The hash mark indicates a hypothetical point at which enough bonds have formed between epoxy and rubber to favor nanoscale over macroscale morphologies. The position of this hash mark should depend on the relative reactivities of the various amine constituents, with a faster reacting rubber shifting the hash mark lower on the arrow. This generalized representation would be the same for resin- and rubber-tuned materials, with $n$ being replaced by $e$ or $R$, respectively.

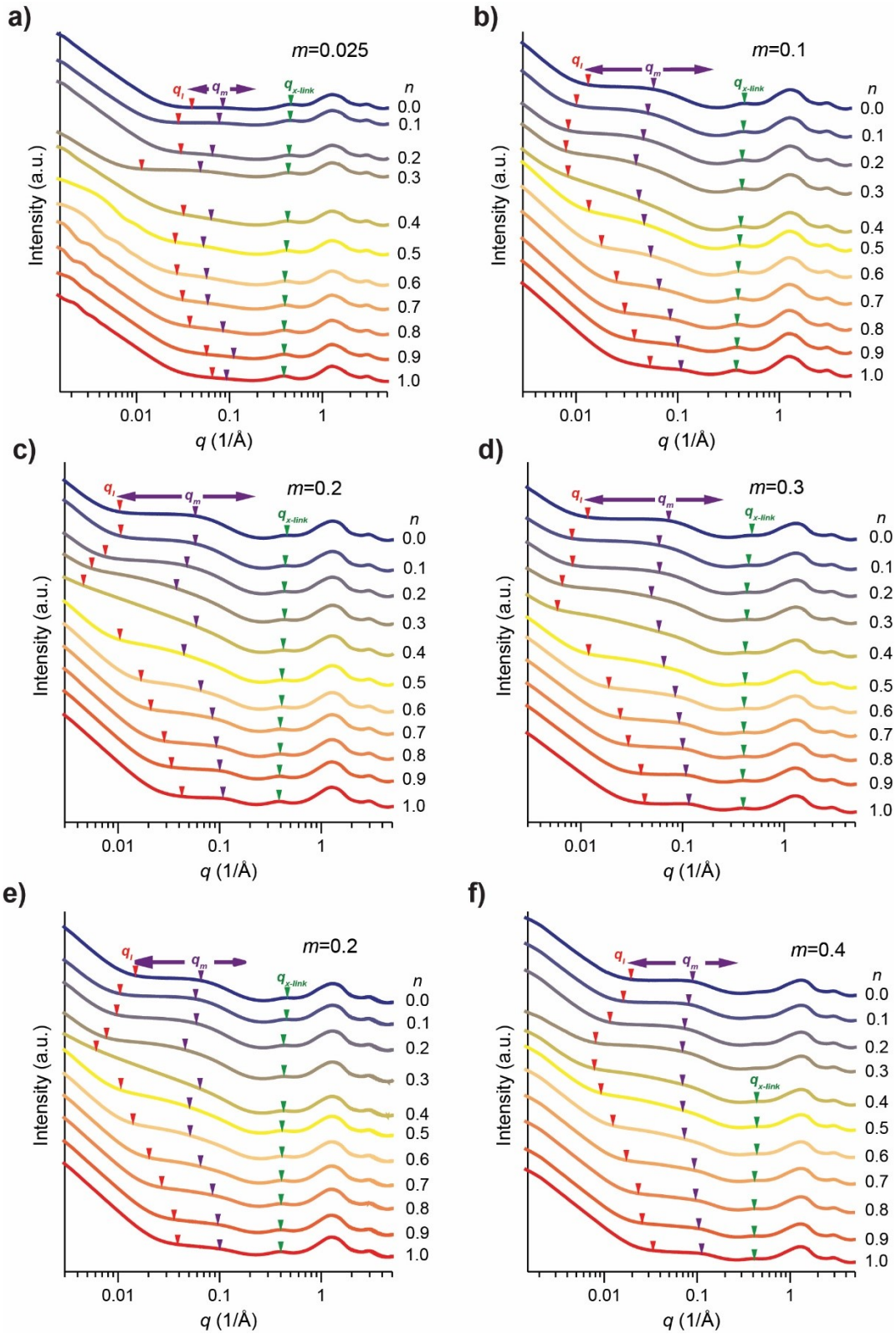
a)
m=0.025
b)
m=0.1
c)
m=0.2
d)
m=0.3
e)
m=0.2
f)
m=0.4
Intensity (a.u.)
q (1/Å)
0.01
0.1
1
n
0.0
0.1
0.2
0.3
0.4
0.5
0.6
0.7
0.8
0.9
1.0

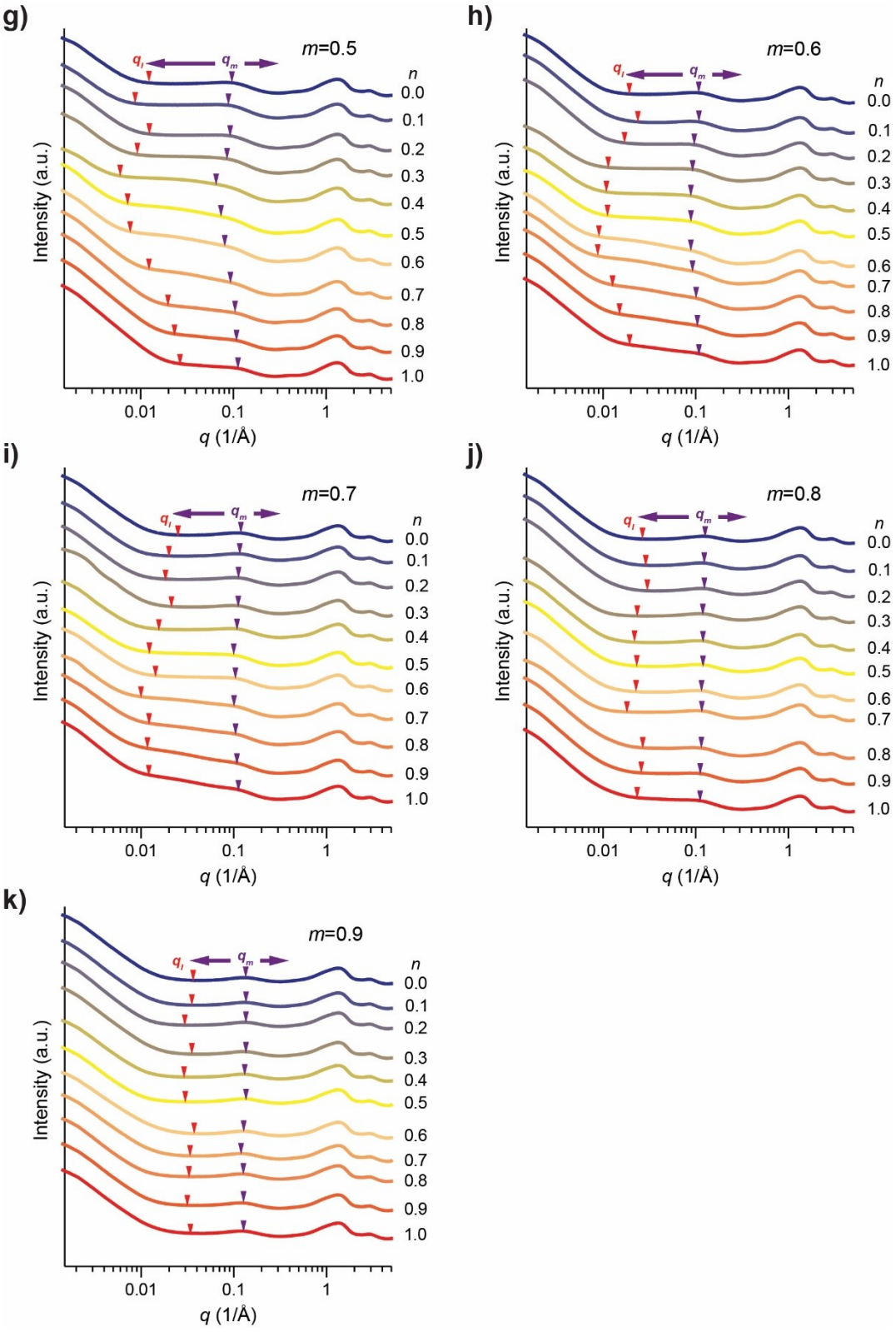


**Figure S2. X-ray scattering of fully cured CA-tuned epoxies**. SWAXS patterns of samples cured at (a-d) 60°C and (e-k) 100°C.

**Table S2.** The longest wavelength of compositional fluctuation, $d_l$, of the ETTD systems with $m$ = 0.025 - 0.3 cured at 60 °C and $m$ =0.2 - 0.9 cured at 100 °C.

| $n$ | $m$ | | | | | | | | | | |
|---|---|---|---|---|---|---|---|---|---|---|---|
| | $d_l$ (nm) of ETTD cured at 60 °C | | | | $d_l$ (nm) of ETTD cured at 100 °C | | | | | | |
| | **0.025** | **0.1** | **0.2** | **0.3** | **0.2** | **0.4** | **0.5** | **0.6** | **0.7** | **0.8** | **0.9** |
| **0.0** | 16.7 | 48.0 | 63.6 | 53.1 | 41.2 | 32.3 | 48.1 | 32.7 | 26.6 | 22.3 | 16.9 |
| **0.1** | 22.8 | 59.1 | 59.1 | 78.1 | 59.2 | 41.8 | 64.3 | 26.9 | 32.0 | 21.9 | 18.1 |
| **0.2** | 21.3 | 77.1 | 85.1 | 74.6 | 63.5 | 52.5 | 49.8 | 37.4 | 35.5 | 21.3 | 21.1 |
| **0.3** | 54.2 | 75.7 | 117.1 | 93.1 | 79.3 | 78.3 | 65.8 | 56.7 | 30.0 | 31.6 | 18.2 |
| **0.4** | 16.8 | 75.2 | 149.8 | 107.5 | 66.1 | 82.9 | 104.0 | 53.5 | 42.4 | 27.9 | 21.3 |
| **0.5** | 23.5 | 48.3 | 61.4 | 51.7 | 56.5 | 67.3 | 88.0 | 54.5 | 51.5 | 26.6 | 22.4 |
| **0.6** | 22.7 | 35.7 | 37.4 | 33.7 | 46.1 | 48.9 | 78.3 | 72.4 | 45.0 | 29.0 | 16.1 |
| **0.7** | 18.4 | 24.8 | 30.8 | 26.2 | 31.2 | 36.9 | 52.5 | 70.6 | 65.8 | 39.5 | 19.7 |
| **0.8** | 15.7 | 22.0 | 22.1 | 21.6 | 23.9 | 28.2 | 32.7 | 49.8 | 51.5 | 24.8 | 23.4 |
| **0.9** | 10.4 | 16.0 | 18.7 | 16.8 | 18.5 | 25.2 | 27.4 | 42.4 | 57.8 | 26.1 | 19.9 |
| **1.0** | 9.0 | 12.0 | 15.1 | 14.8 | 16.7 | 19.0 | 24.3 | 33.5 | 51.5 | 27.6 | 18.2 |

**Table S3.** The wavelength of compositional fluctuation, $d_m$, of the ETTD systems with $m$ = 0.025 - 0.3 cured at 60 °C and $m$ =0.2 - 0.9 cured at 100 °C.

| $n$ | $m$ | | | | | | | | | | |
|---|---|---|---|---|---|---|---|---|---|---|---|
| | $d_m$ (nm) of ETTD cured at 60 °C | | | | $d_m$ (nm) of ETTD cured at 100 °C | | | | | | |
| | **0.025** | **0.1** | **0.2** | **0.3** | **0.2** | **0.4** | **0.5** | **0.6** | **0.7** | **0.8** | **0.9** |
| **0.0** | 7.4 | 10.8 | 10.9 | 8.6 | 9.6 | 7.1 | 6.5 | 5.8 | 5.3 | 4.9 | 4.7 |
| **0.1** | 8.1 | 12.3 | 10.8 | 10.6 | 10.8 | 7.7 | 7.1 | 5.8 | 5.4 | 5.1 | 4.7 |
| **0.2** | 9.6 | 13.6 | 13.2 | 10.7 | 10.7 | 8.6 | 6.8 | 6.5 | 5.6 | 5.1 | 4.7 |
| **0.3** | 12.9 | 16.1 | 16.7 | 12.7 | 13.7 | 9.0 | 7.4 | 6.8 | 5.6 | 5.3 | 4.7 |
| **0.4** | 15.6 | 15.1 | 10.7 | 10.7 | 9.8 | 9.0 | 9.7 | 7.1 | 5.8 | 5.3 | 4.8 |
| **0.5** | 18.8 | 13.4 | 14.0 | 9.6 | 12.4 | 9.0 | 8.6 | 7.1 | 6.3 | 5.3 | 4.7 |
| **0.6** | 17.4 | 11.6 | 9.6 | 7.4 | 12.3 | 8.6 | 7.7 | 7.1 | 6.0 | 5.4 | 4.9 |
| **0.7** | 16.9 | 9.6 | 7.4 | 6.8 | 9.7 | 6.8 | 6.8 | 6.8 | 6.3 | 5.4 | 5.3 |
| **0.8** | 11.8 | 7.4 | 6.8 | 6.3 | 7.4 | 6.5 | 6.0 | 6.3 | 6.0 | 5.4 | 4.9 |
| **0.9** | 8.9 | 6.3 | 6.3 | 5.8 | 6.5 | 6.0 | 5.8 | 6.0 | 5.8 | 5.6 | 4.9 |
| **1.0** | 10.8 | 5.8 | 5.8 | 5.4 | 6.3 | 5.6 | 5.6 | 5.8 | 5.6 | 5.6 | 4.9 |

**Table S4.** The wavelength of crosslink, $d_{x\text{-}link}$, of the ETTD systems with $m$ = 0.025 - 0.3 cured at 60 °C and $m$ =0.2 - 0.9 cured at 100 °C.

| $n$ | $m$ | | | | | | | | | | |
|---|---|---|---|---|---|---|---|---|---|---|---|
| | $d_{x\text{-}link}$ (nm) of ETTD cured at 60 °C | | | | $d_{x\text{-}link}$ (nm) of ETTD cured at 100 °C | | | | | | |
| | **0.025** | **0.1** | **0.2** | **0.3** | **0.2** | **0.4** | **0.5** | **0.6** | **0.7** | **0.8** | **0.9** |
| **0.0** | 1.4 | 1.38 | 1.36 | - | 1.4 | - | - | - | - | - | - |
| **0.1** | 1.4 | 1.41 | 1.42 | 1.4 | 1.4 | - | - | - | - | - | - |
| **0.2** | 1.4 | 1.44 | 1.44 | 1.5 | 1.4 | - | - | - | - | - | - |
| **0.3** | 1.5 | 1.46 | 1.46 | 1.5 | 1.5 | - | - | - | - | - | - |
| **0.4** | 1.5 | 1.5 | 1.48 | 1.5 | 1.5 | 1.4 | - | - | - | - | - |
| **0.5** | 1.5 | 1.54 | 1.53 | 1.5 | 1.5 | 1.4 | - | - | - | - | - |
| **0.6** | 1.6 | 1.55 | 1.54 | 1.5 | 1.5 | 1.4 | - | - | - | - | - |
| **0.7** | 1.6 | 1.6 | 1.58 | 1.6 | 1.5 | 1.5 | - | - | - | - | - |
| **0.8** | 1.6 | 1.63 | 1.58 | 1.6 | 1.6 | 1.5 | - | - | - | - | - |
| **0.9** | 1.62 | 1.63 | 1.62 | 1.6 | 1.57 | 1.53 | - | - | - | - | - |
| **1.0** | 1.63 | 1.67 | 1.63 | 1.6 | 1.57 | 1.53 | - | - | - | - | - |

**Table S5.** The wavelength of composition fluctuation, $d_l$ and $d_m$, and crosslink, $d_{x\text{-}link}$, of epoxy resin-tuned samples with $m$ = 0.1.

| $n$ | $d_l$ (nm) | $d_m$ (nm) | $d_{x\text{-}link}$ (nm) |
|---|---|---|---|
| **0.0** | 30.59 | 9.75 | 2.51 |
| **0.1** | 47.28 | 10.69 | 2.59 |
| **0.2** | 51.54 | 12.20 | 2.51 |
| **0.3** | 67.34 | 15.02 | 2.27 |
| **0.4** | 85.37 | 17.82 | 2.15 |
| **0.5** | 184.80 | 29.64 | 1.88 |
| **0.6** | 100.37 | 15.51 | 1.83 |
| **0.7** | 65.79 | 15.67 | 1.75 |
| **0.8** | 45.04 | 13.65 | 1.67 |
| **0.9** | 29.64 | 10.69 | 1.65 |
| **1.0** | 18.51 | 8.55 | 1.65 |

**Table S6.** The wavelength of composition fluctuation, $d_l$ and $d_m$, and crosslink, $d_{x\text{-}link}$, of rubber-tuned samples with $m$ = 0.1.

| $n$ | $d_l$ (nm) | $d_m$ (nm) | $d_{x\text{-}link}$ (nm) |
|---|---|---|---|
| **0.0** | - | - | 1.63 |
| **0.1** | 13.72 | 7.39 | 1.63 |
| **0.2** | 15.42 | 7.39 | 1.63 |
| **0.3** | 19.39 | 7.74 | 1.63 |
| **0.4** | 19.93 | 8.13 | 1.63 |
| **0.5** | 21.76 | 8.13 | 1.65 |
| **0.6** | 18.16 | 8.13 | 1.63 |
| **0.7** | 18.05 | 8.13 | 1.63 |
| **0.8** | 18.16 | 8.13 | 1.63 |
| **0.9** | 18.88 | 8.13 | 1.63 |
| **1.0** | 27.12 | 9.62 | 1.63 |

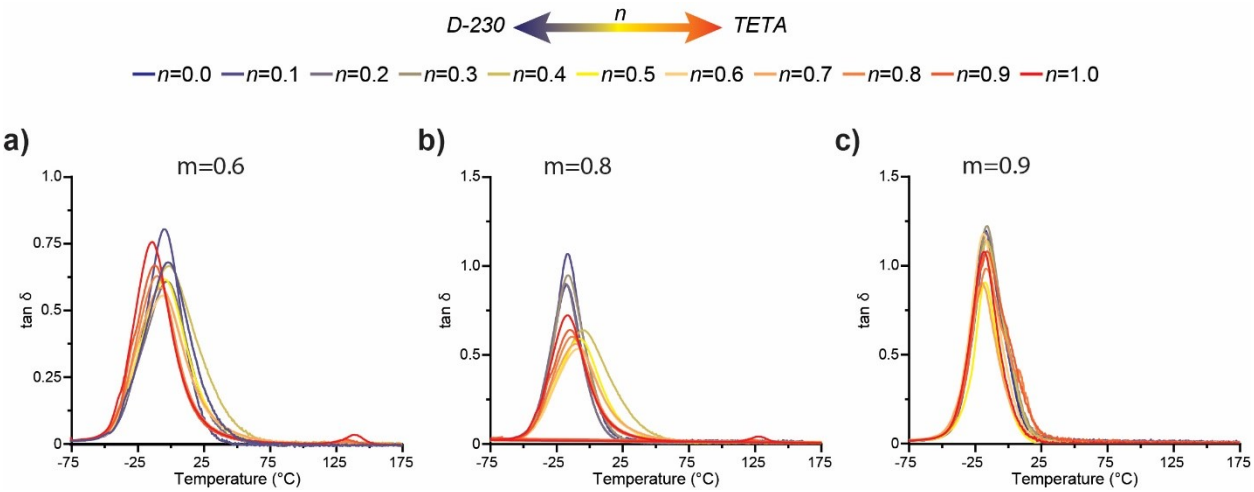


**Figure S2.** Loss tangent vs. temperature for DGEBA-T3000-TETA-D230 networks formulated with *m*=0.6, 0.8 and 0.9 and varying *n* from 0 to 1 cured at 100°C. For this system, $m=[-NH-]_{0,T3000}/[-NH-]_{0,total}$ and $n=[-NH-]_{0,TETA}/([-NH-]_{0,TETA} + [-NH-]_{0,D230}$.

1. S. C. Leguizamon, J. Powers, J. Ahn, S. Dickens, S. L. Lee and B. H. Jones, *Macromolecules*, 2021, **54**, 7796–7807.